Investigation on the Cell Nucleation and Cell Growth in Microcellular Foaming by Means of Temperature Quenching

Xinghua Sun, Huiju Liu, Gang Li, Xia Liao, Jiasong He

State Key Laboratory of Engineering Plastics, Center for Molecular Science, Institute of Chemistry, The Chinese Academy of Sciences, Beijing 100080, China

Received 29 July 2003; accepted 15 February 2004
DOI 10.1002/app.20445
Published online in Wiley InterScience (www.interscience.wiley.com).

ABSTRACT: The cell nucleation and real-time cell growth with increasing cell growth time in microcellular foaming were investigated by means of temperature quenching in a supercritical CO_2 pressure-quench process. Samples of uniform size and shape were saturated in a vessel under conditions of 100–180°C and 30 MPa, and then depressurized to the atmosphere in 10 s. After depressurization, these samples were removed from the vessel at prescribed intervals, and immediately immersed in an ice-water slurry to obtain foamed samples with various cell growth times. It was found that the nucleation density is closely correlated to the gas absorption capacity of the polymer matrix, so that the final cell density should not be adopted as the nucleation density, as done commonly. The change of cell structure and mass density with increasing cell growth time was dominated by gas diffusion behavior, which was strongly influenced by the temperature. The final cell structure was mainly determined by the cell growth step, where gas diffusion played a key role. The final cell density was in direct proportion to the gas remaining in the substrate, which ranged from 6.0×10^9 to 4.7×10^6 cells/cm^3. © 2004 Wiley Periodicals, Inc. J Appl Polym Sci 93: 163–171, 2004

Key words: microcellular foaming; supercritical CO_2; nucleation; growth; structure

INTRODUCTION

Microcellular foaming of glassy polymers with carbon dioxide or nitrogen as a physical-blowing agent was first described by Martini and coworkers.[1] In general, microcellular polymers are characterized by a cell size of about 10 μm and a cell density between 10^9 and 10^{15} cells/cm^3. This kind of novel materials has been the focus of increased attention in the past two decades because of its unique ability to offer a new range of insulating and mechanical properties with reduction in material costs.[2–4] Previous studies revealed that microcellular polymers have the properties of high impact strength,[5,6] high toughness,[7] high stiffness-to-weight ratio,[8] high thermal stability,[9] low dielectric constant,[10] and low thermal conductivity.[11] Thus, microcellular polymers find many potential applications such as food packaging, refrigerator linings, and sporting equipment, for example. Moreover, the tiny size and uniform distribution of the microvoids make it possible to produce small-profile foaming parts for insulating purposes, such as microelectronic circuit board insulators, electronic signal wire insulation, and read-only memory storage, which cannot be produced in traditional foaming processing.[12]

Several techniques have been developed to prepare microcellular polymers by using gases in their supercritical and nonsupercritical states as physical blowing agents. All these techniques rely on the same principles: (1) the polymer is saturated with a gaseous penetrant (blowing agent) at high pressure; (2) the polymer/gas mixture is quenched into a supersaturated state by either reducing pressure or increasing temperature; and (3) nucleation and growth of gas cells dispersed throughout the polymer sample evolve until all thermodynamic forces driving mass transport vanish. Thermoplastic polymers can be foamed by using a continuous extrusion method. In this process, the gas is fed into an extruder and mixed with the polymeric melt at elevated temperatures and pressures. The polymer/gas mixture subsequently foams once it passes the die of the extruder. Noncontinuous foaming techniques have been used as well, in which two alternatives should be distinguished here. The first is a heating process, which starts with saturating the polymer at a temperature below the glass-transition temperature of the mixture. After removing the saturated polymer from the high-pressure vessel, it is foamed in a rapid heating step at temperatures above the glass-transition temperature of the mixture. The second is a pressure-quenching process, which starts with saturating the polymer with the gas at tempera-

Correspondence to: J. He (hejs@sklep.icas.ac.cn).
Contract grant sponsor: National Natural Science Foundation of China; contract grant number: 59873026.

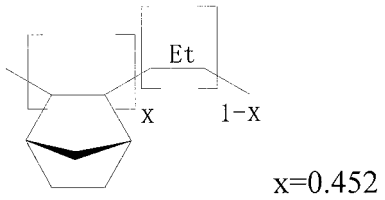

Figure 1 Chemical structure of cyclic olefin copolymer (COC).

tures above the glass-transition temperature of the mixture. Then a microcellular structure is obtained by quenching the pressure, either instantaneously or at a controlled rate. The second alternative is the closest one physically to the continuous method, and thus it is usually adopted to investigate the mechanism of microcellular foaming.[13]

The main advance in making microcellular polymers in the 1990s is the application of supercritical fluids (SCFs), not only in the batch process but also in the traditional continuous process such as extrusion and injection molding.[14–16] It has been found that, by using SCFs as the foaming agent, time is saved in the saturation step, so that this new technique can be used in industrial processes. In making microcellular polymers, supercritical CO_2 was chosen as the foaming agent because of its easily attainable critical parameters (T_c = 31.05°C, P_c = 7.286 MPa) as well as nontoxic, nonflammable character, and commercially available high purity. When polymers are saturated by supercritical CO_2, the glass-transition temperature can be depressed to room temperature in the case of poly(methyl methacrylate), and the same for polystyrene, poly(vinyl chloride), and bisphenol-A polycarbonatePC.[17]

The investigation of cell nucleation and cell growth is vital to the understanding of the mechanism dominating microcellular foaming as well as the effect of processing parameters on cell structures. The aforementioned method was to simulate the process numerically according to Colton's classical nucleation theory[18] and cell growth model,[19] then to compare the results with the final stable cell parameters.[20–24] Although the monitoring of cell formation process is undoubtedly of great importance to the control of cell structures in continuous processing, the study of real nucleation density and change of cell structures with cell growth time has not been reported in the literature. Therefore, in the present article we will introduce a technique to acquire nucleation density and real-time cell parameters in the course of the cell growth step. The adopted method for preparing microcellular polymer is pressure quenching by using supercritical CO_2 as a blowing agent. Cell nucleation, cell growth, and their relationships to gas absorption capacity and gas diffusion are investigated in detail.

EXPERIMENTAL

Materials

A cyclic olefin copolymer (COC) was received from a collection of IUPAC WP EA Task Group (1999-039-1-400; Research Triangle Park, NC). Such a COC was chosen because of its good processability and appropriate T_g compared with that of other COCs. Its chemical structure and properties are shown in Figure 1 and Table I, respectively. Carbon dioxide (99.95% purity) was supplied by Beijing Huayuan Gas Inc. (China). The copolymer was dried at 80°C under vacuum for 24 h before melt processing. Then it was injection molded at 225°C (dimensions: 1.54 mm thick; 15.4 mm wide) on a CS-183 Mini-Max injection-molding instrument.

Foam preparation

The molded polymer plates were cut into bars (1.54 × 2.0 × 15.4 mm). Ten samples of the above uniform size and shape were placed in aluminum tubes, one in each. All the tubes were placed in a high-pressure vessel. The vessel was flushed with low-pressure CO_2 for about 3 min and preheated to a scheduled temperature (100–180°C). Then the pressure was increased to 30 MPa and maintained for a sufficient time to ensure equilibrium absorption of CO_2 by the sample. The equilibrium time of CO_2 absorption was determined by the method of McCarthy.[25] After saturation, a rapid quench of pressure to atmosphere was adopted in 10 s (the temperature fluctuation of the vessel is <2°C during depressurization, as indicated on the panel of temperature controller), followed by cell growth of foaming samples in the vessel at the saturating temperature. Then the tubes with samples were removed from the vessel, one at each scheduled interval (the shortest removal time was 7 s), and immediately placed in an ice-water slurry to stop cell growth. The whole vessel with the remaining tubes was kept at the saturating and foaming temperature until all the tubes were removed. Because all the samples had uniform size and shape, and were foamed in the same vessel under the same circumstance, it was considered that they had identical cell formation behavior. Their only difference was the different time for their cell growth. Thus, cell structures having various cell growth times were obtained.

TABLE I
Properties of Cyclic Olefin Copolymer (COC)

T_g (°C)	M_n × 10^{-4}	M_w × 10^{-4}	M_z × 10^{-4}	M_w/M_n	Density (g/cm^3)
137	6.29	10.99	17.82	1.75	1.02

Foam characterization

The foamed samples were fractured in liquid nitrogen, coated with an approximately 10 nm thick layer of gold on the fractured surface, and observed with a KYKY 1000-B scanning electron microscope (Chinese Academy of Sciences, Beijing, China). The cell diameters and cell densities were characterized using the method of Kumar and Suh.[26] The cell diameter (D) is the average of all the cells in the SEM micrograph, and usually more than 100 cells were measured. The cell density (N_f), which is the number of cells per cubic centimeter of foam, was calculated as

$$N_f = \left(\frac{nM^2}{A}\right)^{3/2} \tag{1}$$

where n is the number of cells seen on the SEM micrograph, A is the area of the micrograph (cm^2), and M is the magnification factor. In addition, the cell density (N_0), based on the pristine unfoamed sample, was calculated as

$$V_f = \frac{\pi}{6} D^3 N_f \tag{2}$$

$$N_0 = \frac{N_f}{1 - V_f} \tag{3}$$

where V_f is the volume fraction occupied by the microvoids. In this article, N_0 was used to compare the cell densities of different foamed samples.

The relative density, which is another important characteristic parameter of foamed polymers, was determined according to ISO 1183-1987. The mass of the sample, in atmosphere and distilled water, was measured by using an analytical balance with an accuracy of 0.1 mg. The density of the sample (d) was calculated as

$$d = \frac{m_{\text{gas}}}{m_{\text{water}}} \rho_{\text{water}} \tag{4}$$

where ρ_{water} is the density of distilled water at room temperature; m_{gas} and m_{water} represent the mass of the sample in atmosphere and in distilled water, respectively. Then the density of the foamed sample was divided by the density of the pristine sample to obtain the relative density.

RESULTS AND DISCUSSION

The whole procedure used for preparing microcellular polymers was a pressure-quench method. It consisted of sample saturation, cell nucleation during depressurization, cell growth after depressurization, and cell growth equilibrium. In previous studies, the cell density after cell growth equilibrium reached was referred to as nucleation density, regardless of the effect of cell growth step on the final cell density. To investigate their relationships, we first compared nucleation density with final cell density after cell growth equilibrium.

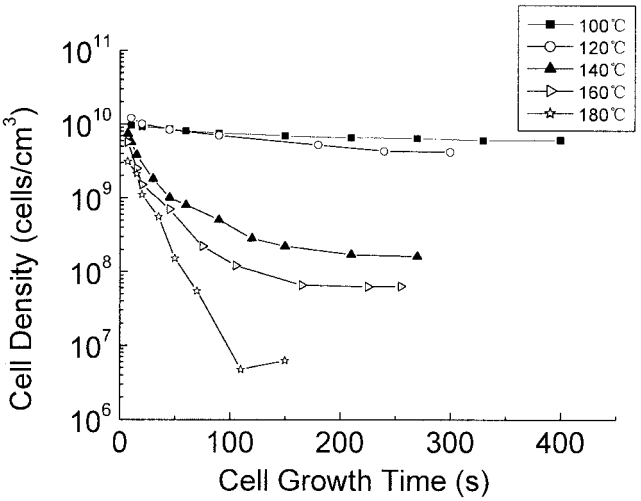

(I)

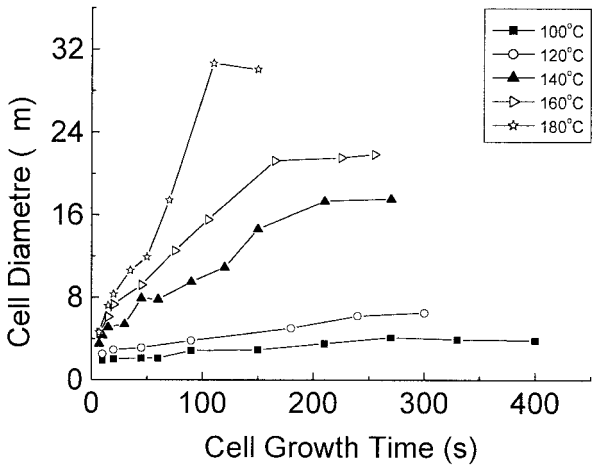

(II)

Figure 2 Cell structures at various cell growth times prepared at P = 30 MPa and depressurization time = 10 s: (I) cell density; (II) cell diameter.

Cell nucleation

Figure 2(I) shows the change of cell density with increasing cell growth time at different test tempera-

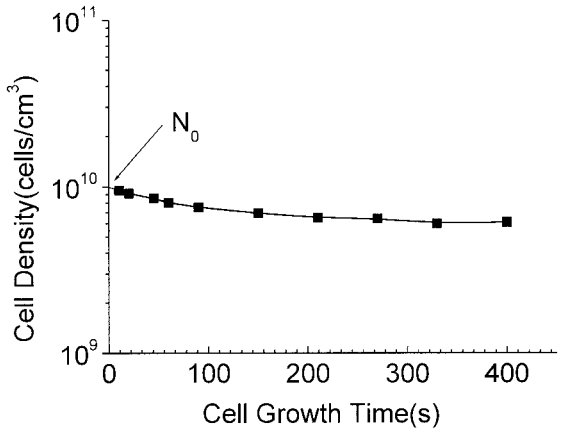

Figure 3 Method of acquiring cell nucleation density.

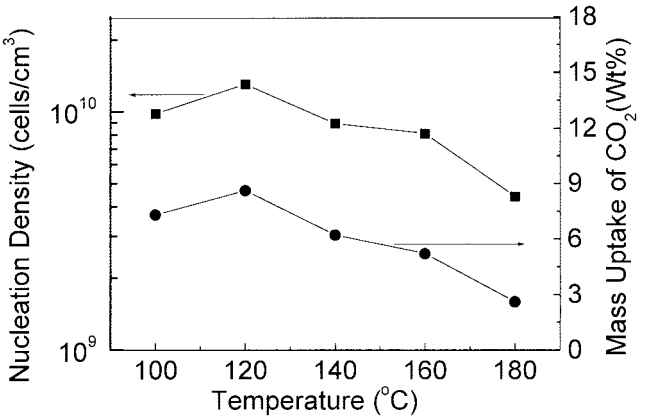

Figure 4 Comparison of nucleation density with equilibrium mass uptake of CO_2 at various temperatures.

tures. According to the shape of curves at the initial stage, the curves of cell density versus cell growth time are linearly extrapolated to zero-time point to acquire a cell density, which indicates the nucleation density formed during the course of depressurization (Fig. 3) at a fixed foaming temperature. According to Colton's classical nucleation theory,[18] the nucleation density is in proportion to the concentration of gas in the substrate in homogeneous nucleation. To investigate the mechanism dominating cell nucleation, the solubility of CO_2 in COC was measured according to McCarthy's method.[25] In their work, McCarthy and colleagues rapidly decompressed supercritical CO_2–saturated polystyrene at sufficiently high temperatures (above the depressed T_g), and immediately transferred the samples to a balance to record mass loss as a function of time. From these measurements, the percentage mass uptakes were calculated and the results plotted versus the square root of desorption time. This yielded linear plots that were indicative of Fickian diffusion kinetics. Linear extrapolation to zero desorption time gave the uptake of CO_2 at the end of the sorption period. Figure 4 shows a comparison of nucleation density with equilibrium mass uptake of CO_2 at various temperatures. It can be seen clearly that both curves first increase with increasing temperature, then decrease with increasing temperature, passing through a maximum at 120°C. Such a similarity signifies that the nucleation density relies qualitatively on the amount of CO_2 dissolved in the sample at the same depressurization rate. Compared to this, other parameters, such as temperature and pressure, have an indirect effect on the cell nucleation density through influencing CO_2 absorption capacity of the sample.

Figure 5 is a comparison of nucleation density (N_n) and final cell density after cell growth equilibrium (N_e). There is only a slight variation in nucleation density at different temperatures, ranging from 1.3 $\times$ 10^{10} to 4.4 $\times$ 10^9 cells/cm^3, although the finally obtained cell density decreases distinctly with increasing temperature, ranging from 6.0 $\times$ 10^9 to 4.7 $\times$ 10^6 cells/cm^3 for 100 and 180°C, respectively. The difference between nucleation density and final cell density grows rapidly with increasing temperature. In previous studies of cell nucleation in microcellular foaming, the effect of cell growth step on the final cell density was neglected and the final cell density was adopted to represent nucleation density.[23,27–32] It is for the first time that such a tremendous difference in nucleation density and final cell density has been reported. It suggests that most of the nuclei formed during the cell nucleation step disappear in the cell growth step at higher temperatures, which should be the nature of the phenomenon that final cell density decreases substantially with increasing temperature. It is concluded in the present work that the final cell density should not be adopted to represent the nucleation density. To further understand the effect of the cell growth step on the final cell structure and the mechanism dominating cell growth, we investigated the real-time change of

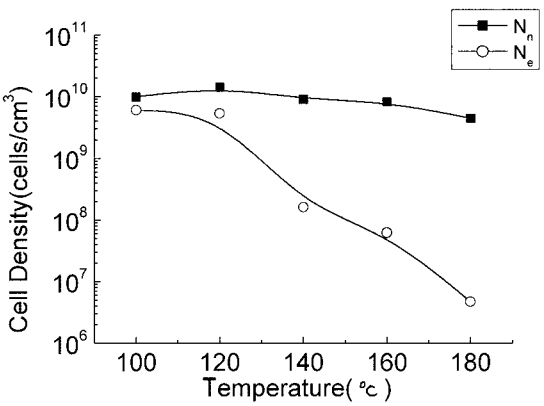

Figure 5 Comparison of nucleation density (N_n) and final cell density (N_e) at various temperatures at P = 30 MPa and depressurization time = 10 s.

cell morphology, cell structures (cell size and cell density), and mass density with increasing cell growth time and its relationship to the diffusivity of gas, discussing these parameters in the following sections.

Cell growth

Cell morphology at various cell growth times

Figures 6 to 8 show the change of cell morphology with cell growth time at 100, 140, and 180°C, respectively. At 100°C (Fig. 6, white bar indicates 10 μm), the cells are isolated spheres, and cell density remains nearly the same at various cell growth times, as shown in Figure 2(I). Figure 7 (white bar indicates 100 μm) shows that at 140°C, accompanying the increase in cell size is a change in the shape of the cells from discrete and spherical cells, through larger elliptical cells, to a structure consisting of impinging and polygonal cells. At 180°C (Fig. 8, white bar indicates 100 μm), the cell structure is irregular with a flowing shape. Obviously unfoamed areas appear in the substrate at the cell growth time of 30 and 90 s, which suggests that large numbers of cell disappeared during the course of cell growth. The increase of the temperature decreases the viscosity of the substrate materials, successively decreases the retraction force restricting cell growth, and increases the diffusivity of CO_2 within the substrate, factors all leading to more rapid cell growth and larger cells. At the same time, the cell density decreases significantly with increasing cell growth time because of the coalescence and disappearance of cells.

Cell structures with increasing cell growth time

The change of cell structure with increasing cell growth time is demonstrated in Figure 2. At these temperatures, the cell density decreases and cell diameter increases with increasing cell growth time. The cell structure tends to level off after a period of cell growth time. The curve of cell density is higher, and the curve of cell diameter is correspondingly lower at lower temperature. In addition, the curves of cell density and cell diameter have similar shapes, with opposite variation direction at the same foaming temperature.

At 100 and 120°C, below the T_g of the pure polymer, the cell density and cell size varied slightly with cell growth time, whereas at 140, 160, and 180°C, above the T_g of the pure polymer, cell size increased and cell density rapidly decreased with increasing cell growth time. At 100°C, cell density and cell diameter varied from 9.5×10^9 cells/cm^3 and 1.9 μm (10 s) to 6.0×10^9 cells/cm^3 and 3.9 μm (330 s), respectively. At 140°C, cell density and cell diameter varied from 7.4×10^9 cells/cm^3 and 3.5 μm (7 s) to 1.6×10^8 cells/cm^3 and 17.5 μm (210 s), respectively, whereas at 180°C, cell density and cell diameter varied from 3.1×10^9 cells/cm^3 and 4.6 μm (7 s) to 4.7×10^6 cells/cm^3 and 30 μm (110 s), respectively. It can be seen that cell structure changes more rapidly at higher temperatures to reach larger cell size and smaller cell density than at lower temperatures, as discussed in the preceding section.

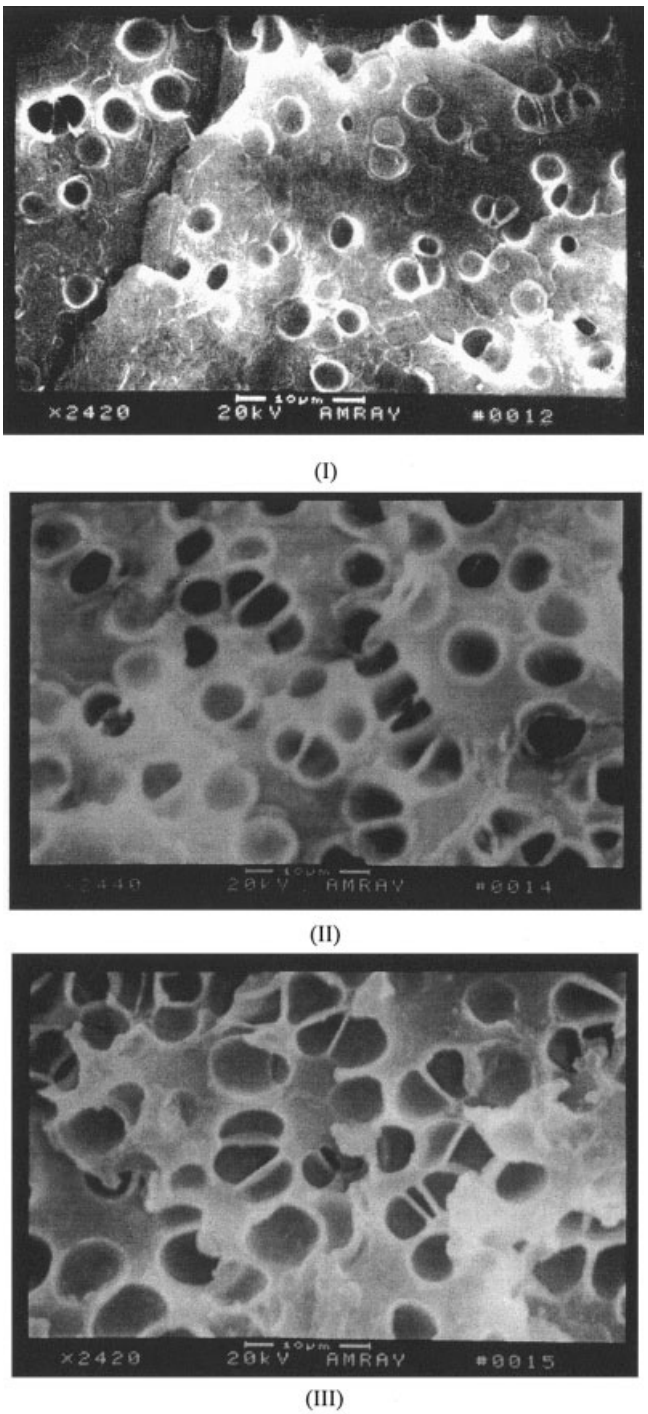

Figure 6 Cell morphology of 100°C at various cell growth times prepared at P = 30 MPa and depressurization time = 10 s: (I) 10 s; (II) 30 s; (III) 90 s.

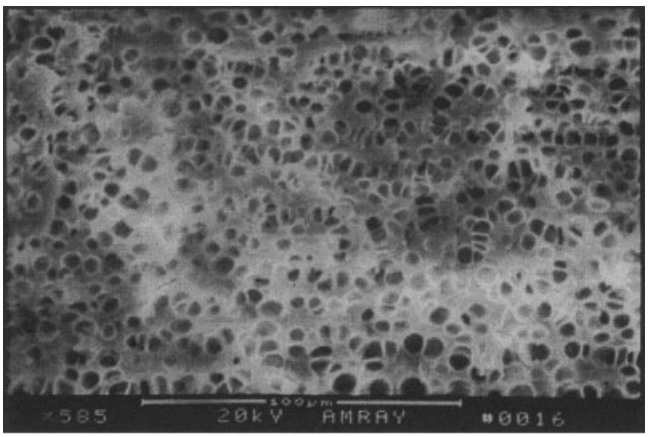

(I)

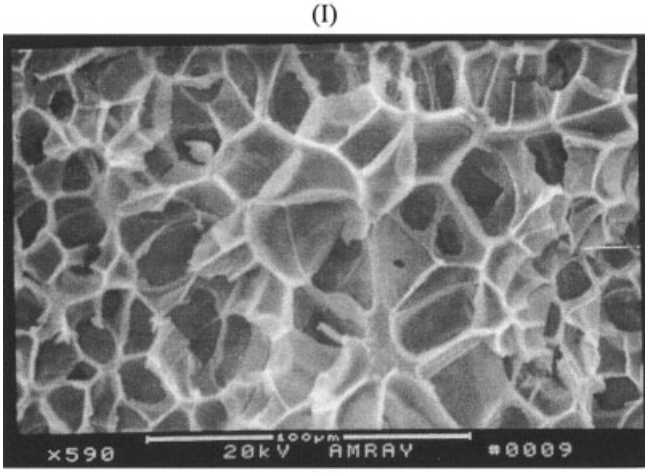

(II)

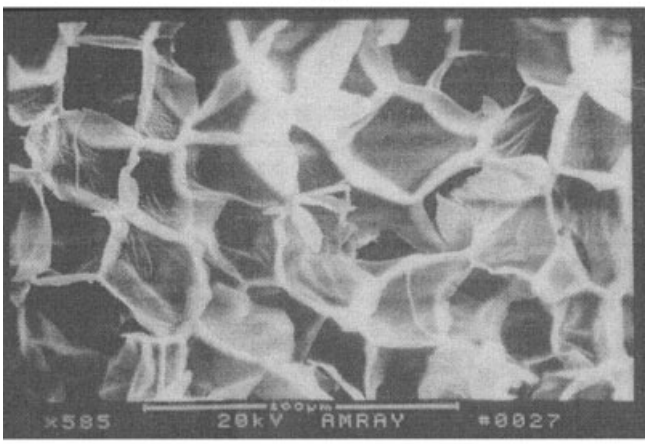

(III)

Figure 7 Cell morphology of 140°C at various cell growth times prepared at P = 30 MPa and depressurization time = 10 s: (I) 7 s; (II) 30 s; (III) 90 s.

Mass density of samples with increasing cell growth time

Figure 9 shows the change of mass density with increasing cell growth time at different temperatures. At temperatures below and near the T_g of the pure polymer (100, 120, 140°C), the mass density first decreases with increasing cell growth time, then levels off after a certain time. This tendency suggests that the absorbed gas mainly diffuses into the nucleated cells at these temperatures, thus causing the substrates to swell, whereas at 160°C, mass density first decreases for a

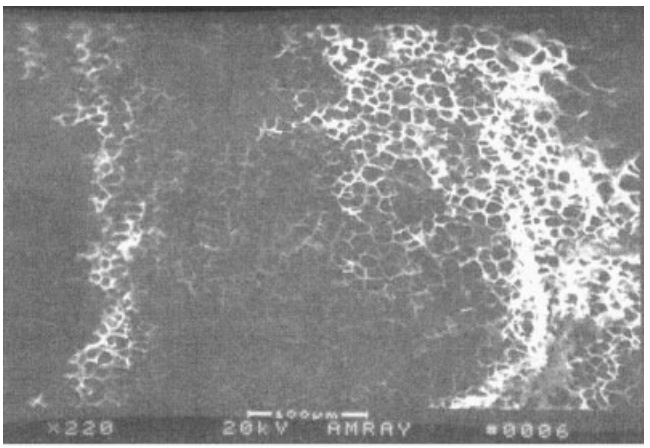

(I)

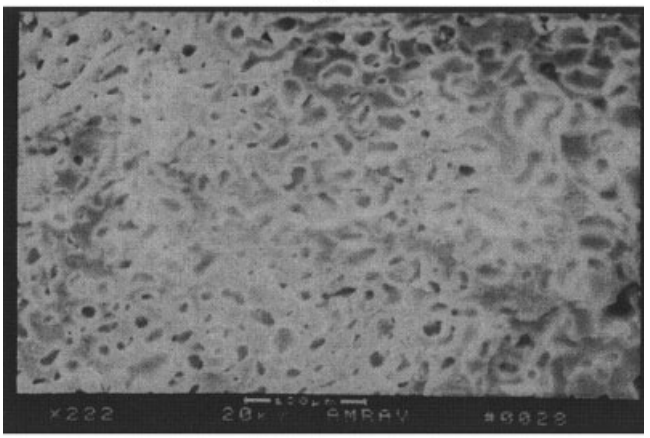

(II)

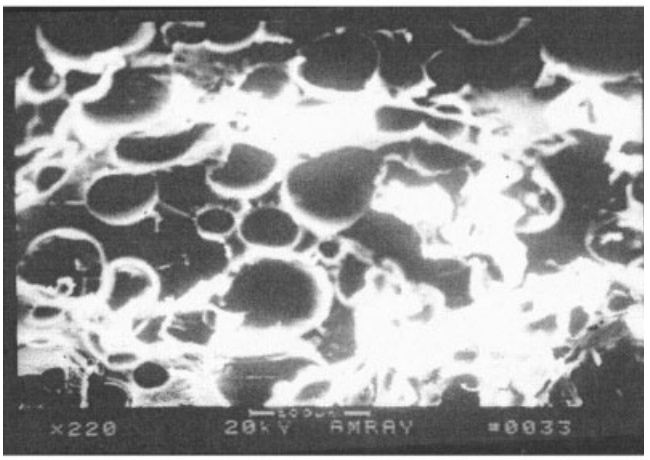

(III)

Figure 8 Cell morphology of 180°C at various cell growth times prepared at P = 30 MPa and depressurization time = 10 s: (I) 7 s; (II) 30 s; (III) 90 s.

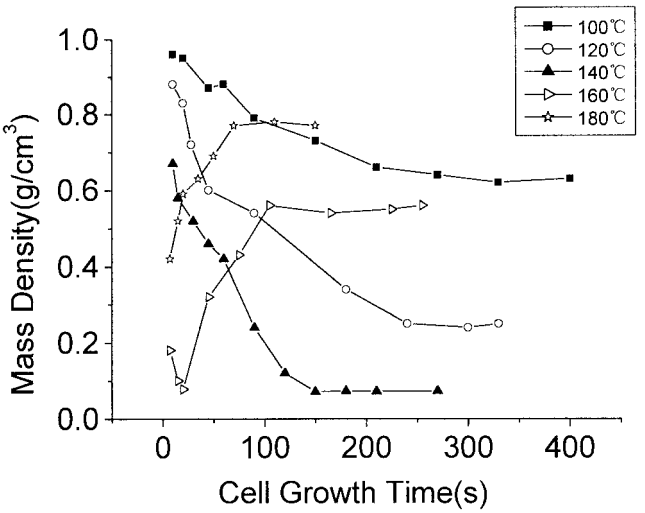

Figure 9 Change of mass density with increasing cell growth time at various temperatures. Foams were prepared at P = 30 MPa and depressurization time = 10 s.

short time, then increases with cell growth time, passing through a minimum. At 180°C, however, such a minimum does not appear, probably because of the overly long removal time (≥7 s). A similar result was reported by Mark,[33] who investigated the effect of foaming time on the relative density of microcellular polysulfone foam at different temperatures in a batch process.

The factors influencing mass density are very complex and ambiguous, such as the amount of gas absorbed, skin thickness, the wall thickness of cells, and cell growth time, for instance.[34] The amount of gas absorbed by the substrate diminishes distinctly with increasing temperatures (Fig. 4), and the gas diffuses out of the substrate with increasing growth time. All these phenomena will lead to an increase in the skin thickness of the sample.[34] Besides, at temperatures far above the T_g of the pure polymer, together with the plasticization of CO_2, the stiffness of the substrate substantially decreases and an abundance of gas diffuses out of the substrate, thus resulting in some completely unfoamed regions (Fig. 10). These factors result in a phenomenon that the mass density first decreases in a short period of time after depressurization, atributed to dominant diffusion of gas into the cells to swell the substrate. Then the mass density increases as a result of the dominant diffusion of gas out of the substrate, causing cells to coalesce and collapse.

Cell growth equilibrium

As shown in Figure 2, the cell diameter and cell density level off nearly at the same time. This time is designated cell growth equilibrium time, at which cells stop growing and cell structure becomes stable.

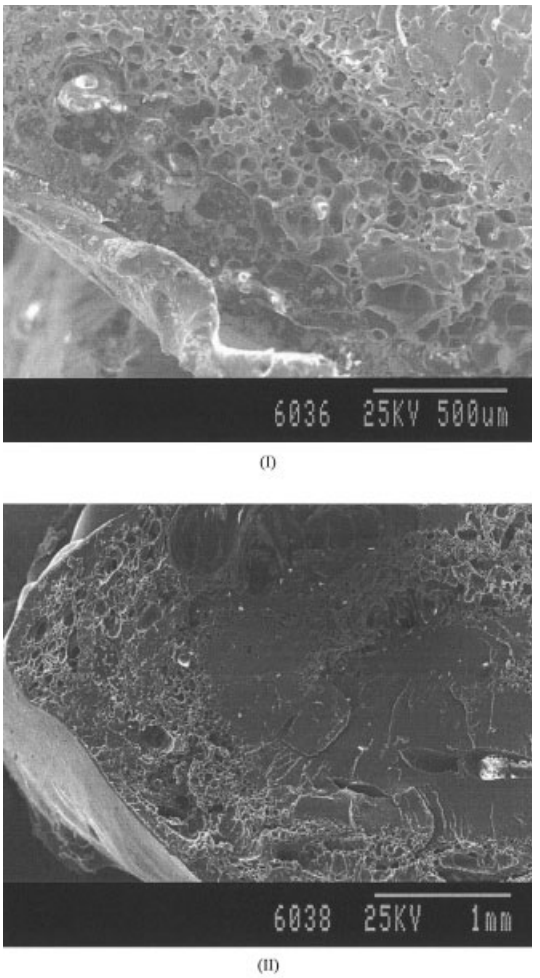

Figure 10 Unfoamed regions in foamed COC samples (T = 180°C, P = 30 MPa, depressurization time = 10 s): (I) cell growth time = 15 s; (II) cell growth time = 50 s.

Figure 11 shows the cell growth equilibrium time at different temperatures. The increase of temperature decreases the viscoelasticity of the polymer matrix and increases the diffusivity of the gas, causing more rapid

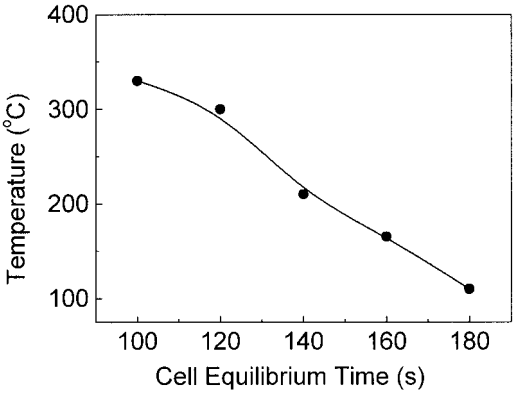

Figure 11 Cell growth equilibrium time at various temperatures at P = 30 MPa and depressurization time = 10 s.

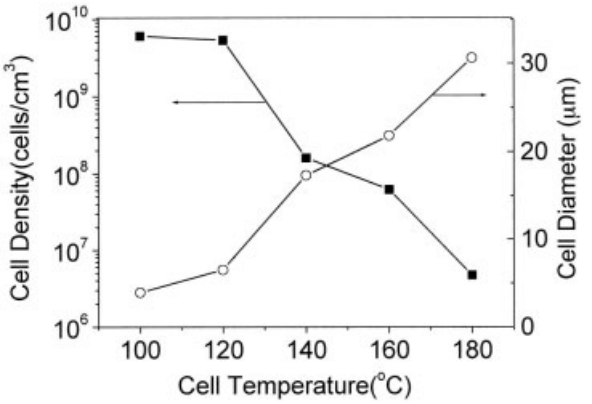

Figure 12 Relationship between the final cell structure and temperature. Foams were prepared at P = 30 MPa and depressurization time = 10 s.

cell growth and shorter cell growth time needed. It takes 330 s for the cell structure to become steady at 100°C, whereas it takes only 110 s at 180°C.

Figure 12 shows the relationship between the final cell structure after cell growth equilibrium time and the foaming temperature. The cell density substantially decreases with increasing temperature, whereas the cell diameter significantly increases with increasing temperature, with an opposite variation trend. At higher temperatures, the lower stiffness of the substrate and higher diffusivity of the gas allow larger cells to grow. Such a result is in accordance with most of the conclusions reported in the study of microcellular foaming.[12,21,25]

In the preceding sections, we investigated real-time cell formation behavior: cell nucleation, cell growth, and cell growth equilibrium. It can be concluded from the above discussion that the final cell density, as well as the corresponding cell diameter, depends on the change of cell structure during cell growth step, not on the nucleation density formed at nucleation step.

Diffusivity of the gas

There are two steps in microcellular processing, cell nucleation and cell growth. According to classical nucleation theory,[18] the main factors influencing cell nucleation include temperature, pressure, depressurization rate, the concentration of the gas in a polymer, and the interface tension of polymer/gas system. The cell growth step is controlled by gas diffusion and stiffness of the substrate.[35,36] The stiffness of the matrix substantially decreases with increasing temperature. To further understand the mechanism dominating cell growth, the diffusion behavior of CO_2 in the substrate was investigated by using the similar method of studying cell growth. About ten samples of uniform size and shape were saturated in the vessel under scheduled circumstances (100–180°C, 30 MPa). The vessel was depressurized to the atmosphere in 10 s, and then the samples were removed, one at each scheduled interval, and weighed immediately with a precision of 0.1 mg. The whole vessel with the remaining samples was kept at the saturating temperature until all the samples were removed. The amount of gas remaining in the substrate at different diffusion times was calculated by this means.

The mass of the remaining gas was divided by that of the pristine polymer to obtain the percentage mass uptake of CO_2 at various diffusion times, which was plotted versus the square root of desorption time. The curve achieved should be a linear one in the initial stage, according to Fickian diffusion kinetics (Fig. 13). However, the linear relationship was not observed at 180°C because of the high diffusion speed of the gas at this temperature. A proper correlation between the curve of CO_2 diffusion (Fig. 13) and that of cell structure (Fig. 2) exists, where the curves become steeper, indicating that less gas finally remains in the substrate at higher temperatures. This diffusion curve appropriately accounts for the change of cell structure and mass density with increasing cell growth time at various temperatures, as well as the relationship of the final cell structure to the temperature. At higher temperatures, increased speed of the gas diffusion together with decreased stiffness of the polymer matrix lead to more rapid growth in the cell diameter and correspondingly more rapid decrease in the cell density. The lower stiffness of the substrate and higher diffusivity of the gas at higher temperatures permit larger cells to form. On the other hand, less gas remains in the substrate at higher temperatures, and thus the final cell density is considerably decreased. As for mass density, the absorbed gas diffuses to <1%

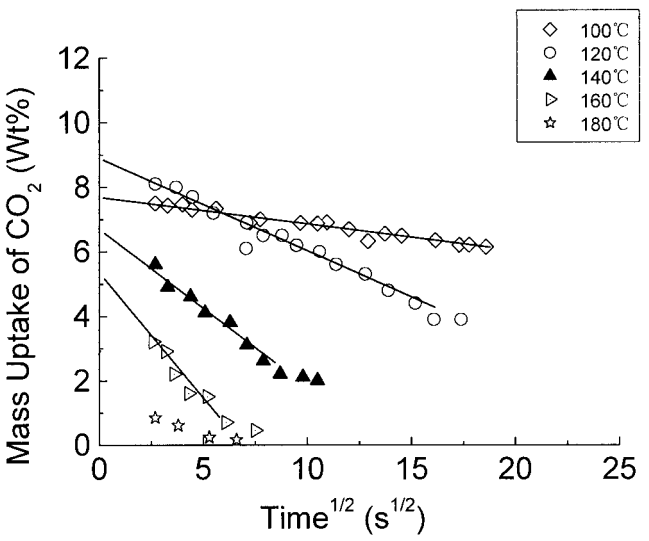

Figure 13 Diffusion behavior of COC/CO_2 system at various temperatures (P = 30 MPa).

mass uptake in 1 min at temperatures of 160 and 180°C, which suggests that the diffusion of the gas out of the substrate and the disappearance of cells dominate. Thus the expansion rate begins to diminish and mass density begins to increase after a short period of time on depressurization (Fig. 9). At temperatures < 140°C, the absorbed gas diffuses slowly, and the remaining mass uptake of the gas is >2%, which suggest that the growth of the cells dominates. Consequently, the mass density of the foamed samples first decreases, then levels off, with increasing time.

CONCLUSIONS

The cell nucleation and cell growth in microcellular foaming were investigated by means of temperature quenching in a supercritical CO_2 pressure-quench process. First, it was found that the final cell structure reached after cell growth equilibrium is determined by the step of cell growth, not by the step of cell nucleation, as suggested in most of the literature. Second, the nucleation density on depressurization depends on the amount of gas absorbed by the polymer matrix in a qualitative way, whereas other processing parameters such as temperature and pressure have an indirect effect on the cell density through influencing the absorption capacity of the substrate. The final cell density should not be adopted to represent the nucleation density. Third, changes of cell morphology, cell structure, and mass density with cell growth time were investigated and it was found that the cell growth step is dominated by the diffusion of the absorbed gas, which increases rapidly with increasing temperatures, causing a distinctly more rapid cell growth at higher temperatures. Finally, the cell growth equilibrium time is inversely proportional to the diffusivity of the gases, with shorter equilibrium time at a higher temperature, where the gas has a larger diffusivity. At higher temperatures, the greater amount of gas diffusing out of substrate and lower stiffness of the polymer matrix in the cell growth step led to a final cell structure with smaller cell density and larger cell diameter.

This work was supported by the National Natural Science Foundation of China, Grant 59873026.

References

1. Martini, J. E. Ph.D. Thesis, Massachusetts Institute of Engineering, Cambridge, MA, 1981.
2. Martini, J. E.; Suh, N. P.; Waldman, F. A. U.S. Pat. 4,473,665, 1984.
3. Kumar, V. Cell Polym 1993, 12, 207.
4. Kumar, V.; Weller, J. E. In: Polymeric Foams: Science and Technology; Khemani, K. C., Ed.; ACS Symposium Series 669; American Chemical Society: Washington, DC, 1997; Chapter 7, pp. 101–114.
5. Martini, J. E.; Waldman, F. A.; Suh, N. P. ANTEC '82, SPE Technical Papers 1982, 28, 674.
6. Collias, D. I.; Baird, D. G.; Borggreve, R. J. M. Polymer 1994, 35, 3978.
7. Baldwin, D. F.; Suh, N. P. ANTEC '92, SPE Technical Papers 1992, 38, 1503.
8. Klempner, D.; Frisch, K. C., Eds. Handbook of Polymeric Foams and Foam Technology; Hanser Publishers: Munich, 1991; Chapter 1.
9. Seeler, K. A.; Kumar, V. J. Reinf Plast Compos 1993, 12, 359.
10. Shimbo, M.; Baldwin, D. F.; Suh, N. P. Polym Eng Sci 1995, 35, 1387.
11. Guria, K. C.; Tripathy, D. K. Int J Polym Mater 1997, 37, 53.
12. Leaversuch, R. D. Mod Plast 2000, 77, 55.
13. Krause, B.; Mettinkhof, R.; van der Vegt, N. F. A.; Wessling, M. Macromolecules 2001, 34, 874.
14. Cha, S. W.; Suh, N. P.; Baldwin, D. F.; Park, C. B. U.S. Pat. 5,158,986, 1992.
15. Baldwin, D. F.; Suh, N. P.; Park, C. B.; Cha, S. W. U.S. Pat. 5,334,356, 1994.
16. Park, C. B.; Suh, N. P. J Manuf Sci Eng 1996, 118, 639.
17. Chiou, J. S.; Barlow, J. W.; Paul, D. R. J Appl Polym Sci 1985, 30, 2633.
18. McHugh, M. A.; Krukonis, V. J. Supercritical Fluid Extraction: Principles and Practice, 2nd ed.; Butterworth-Heinemann: Oxford, UK, 1994; Chapter 1.
19. Bellinger, M. A.; Sauer, J. A.; Hara, M. Macromolecules 1994, 27, 6147.
20. Goel, S. K.; Beckman, E. J. AIChE J 1995, 41, 357.
21. Goel, S. K.; Beckman, E. J. In: Generation of Microcellular Polymers Using Supercritical CO_2, Cellular Polymers II, Proceedings of the 2nd International Conference; Rapra Technology Ltd.: Edinburgh, 1993; Paper 5, pp. 1–11.
22. Goel, S. K.; Beckman, E. J. Cell Polym 1993, 12, 251.
23. Goel, S. K.; Beckman, E. J. Polym Eng Sci 1994, 34, 1137.
24. Goel, S. K.; Beckman, E. J. Polym Eng Sci 1994, 34, 1148.
25. Arora, K. A.; Lesser, A. J.; McCarthy, T. J. Macromolecules 1998, 31, 4614.
26. Kumar, V.; Suh, N. P. Polym Eng Sci 1990, 30, 1323.
27. Colton, J. S.; Suh, N. P. Polym Eng Sci 1987, 27, 485.
28. Colton, J. S.; Suh, N. P. Polym Eng Sci 1987, 27, 493.
29. Colton, J. S.; Suh, N. P. Polym Eng Sci 1987, 27, 500.
30. Kumar, V.; Weller, J. E.; Montecillo, R. J. Vinyl Technol 1992, 14, 191.
31. Kumar, V.; Weller, J. E. J Eng Ind 1994, 116, 413.
32. Baldwin, D. F.; Park, C. B.; Suh, N. P. Polym Eng Sci 1996, 36, 1437.
33. Sun, H. L.; Mark, J. E. J Appl Polym Sci 2002, 86, 1692.
34. Weller, J. E.; Kumar, V. On the Skin Thickness of Microcellular Foams: The Effect of Foaming Temperature. ANTEC '97 1997, 43, 2037.
35. Park, C. B.; Baldwin, D. F.; Suh, N. P. Polym Eng Sci 1995, 35, 432.
36. Wang, J.; Cheng, X. G.; Zheng, X. J.; Yuan, M. J.; He, J. S. J Polym Sci Part B: Polym Phys 2003, 41, 368.